Superparamagnetic gadonanotubes are high-performance MRI contrast agents†

B. Sitharaman,[a] K. R. Kissell,[a] K. B. Hartman,[a] L. A. Tran,[a] A. Baikalov,[b] I. Rusakova,[b] Y. Sun,[b] H. A. Khant,[c] S. J. Ludtke,[c] W. Chiu,[c] S. Laus,[d] É. Tóth,[d] L. Helm,[d] A. E. Merbach[d] and L. J. Wilson*[a]

Received (in Cambridge, UK) 31st March 2005, Accepted 27th May 2005
First published as an Advance Article on the web 8th July 2005
DOI: 10.1039/b504435a

We report the nanoscale loading and confinement of aquated $Gd^{3+}{}_n$-ion clusters within ultra-short single-walled carbon nanotubes (US-tubes); these $Gd^{3+}{}_n$@US-tube species are linear superparamagnetic molecular magnets with Magnetic Resonance Imaging (MRI) efficacies 40 to 90 times larger than any Gd^{3+}-based contrast agent (CA) in current clinical use.

Contrast agents (CAs) play a prominent role in magnetic resonance imaging in medicine.[1] MRI CAs are primarily used to improve disease detection by increasing sensitivity and diagnostic confidence. There are several types of MR contrast agents being used in clinical practice today. These include extracellular fluid space (ECF) agents, extended residence intravascular blood pool agents, and tissue(organ)-specific agents. Annually, approximately sixty million MRI procedures are performed worldwide and around 30% of these procedures use MRI CAs. The lanthanide ion, Gd^{3+}, is usually chosen for MRI CAs because it has a very large magnetic moment ($\mu^2 = 63\ \mu_B{}^2$) and a symmetric electronic ground state, ${}^8S_{7/2}$. The aquated Gd^{3+} ion is toxic and hence is sequestered by chelation[2] or encapsulation[3,4] in order to reduce toxicity.

Single-walled carbon nanotubes (SWNTs) possess unique characteristics that make them desirable for biomedical applications.[5] The ideal length for medical applications is uncertain, but ultra-short nanotubes (20–100 nm) or US-tubes[6,7] are probably best suited for cellular uptake, biocompatibility, and eventual elimination from the body. Additionally, the US-tube exterior surface provides a versatile scaffold for attachment of chemical groups for solubilizing or targeting purposes, while its interior space allows for encapsulation of atoms, ions, and even small molecules[7,8] whose cytotoxicity may be sequestered within the short carbon nanotube. Finally, medical imaging agents derived from US-tubes hold promise for intracellular imaging, since carbon nanotubes have been shown to translocate into the interior of cells with minimal cytotoxicity.[9,10]

In this communication, US-tubes have been explored as "nanocapsules" for MRI-active Gd^{3+} ions. Here, we report the internal loading of US-tubes with aqueous $GdCl_3$ and the characterization of the resulting $Gd^{3+}{}_n$@US-tube species, with their superparamagnetic metal-ion clusters, as powerful proton relaxation centers with relaxivities 40 to 90 times larger than current clinical agents. As such, gadonanotubes introduce a new paradigm for high-performance MRI CA design.

The SWNTs used were produced by the electric arc discharge technique (Carbolex Inc.), with Y/Ni as the catalyst.[11] As-received SWNTs were then cut into US-tubes by fluorination followed by pyrolysis at 1000 °C under an inert atmosphere.[5] The US-tubes were then loaded by soaking and sonicating them in HPLC grade DI water (pH = 7) containing aqueous $GdCl_3$. The experimental details are given in the Supplementary Information. For the relaxivity measurements, a saturated solution of 40 mg of the $Gd^{3+}{}_n$@US-tubes in 20 ml of a 1% sodium dodecyl benzene sulfate (SDBS) aqueous solution and another of 10 mg of the $Gd^{3+}{}_n$@US-tubes in 5 ml of a 1% biologically-compatible pluronic F98 surfactant solution were prepared. Approximately 10% of the $Gd^{3+}{}_n$@US-tubes dispersed and formed a stable suspension. These two supernatant (suspensions) solutions were then used for the relaxometry experiments.

Fig. 1a shows a structural depiction of a single US-tube loaded with Gd^{3+} ions. Gd^{3+}-ion loading may occur through the side-wall defects or end-of-tube openings created by cutting full-length SWNTs into shortened US-tubes.[5] Fig. 1b displays a HRTEM image of the aquated Gd^{3+} ions, apparently inside bundled US-tubes. The extremely large proton relaxivities of these bundled $Gd^{3+}{}_n$@US-tubes (see below) also indicate a highly unusual environment for the Gd^{3+} ions within the US-tubes. The mean particle size of each of the $Gd^{3+}{}_n$@US-tube bundles is 20–80 nm long and 3–10 nm thick from the Cryo-TEM image in Fig. 1c. The HRTEM image revealed that the Gd^{3+} ions are not uniformly distributed, but are present as (1 nm × 2–5 nm) $Gd^{3+}{}_n$-ion clusters (dark spots) at different sites, again apparently within the US-tube bundles. The identification of many of the Gd^{3+}-ions clusters was verified by multiple EDS probings. Assuming that Gd^{3+}-ion loading is mainly through the side-wall defects created by the fluorination cutting procedure, the locations of the $Gd^{3+}{}_n$-ion clusters, in effect, map the locations of these defects whose dimensions, in turn, probably limit the $Gd^{3+}{}_n$-ion cluster sizes.[12] Assuming a cluster size of (1 nm × 2–5 nm) and hydrated $Gd^{3+}{}_n$-ion and Cl^- ions of 0.75 nm and 0.18 nm, respectively, it can be estimated that each $Gd^{3+}{}_n$-ion cluster contains fewer than ten $Gd^{3+}{}_n$ ions.

The XRD powder pattern of a $Gd^{3+}{}_n$@US-tube sample (Supplementary, Fig. S1) indicated only two small peaks from carbon, with no diffraction peaks due to crystalline Gd^{3+}-ion centers. However, the XPS spectrum shown in (Supplementary Fig. S2) clearly demonstrated the presence of Gd^{3+} in the sample,

[a]*Department of Chemistry, the Center for Nanoscale Science and Technology, and the Center for Biological and Environmental Nanotechnology MS 60, Rice University, Houston, Texas, 77251-1892, USA. E-mail: durango@rice.edu; Fax: 713-348-5155; Tel: 713-348-3268*
[b]*The Texas Center for Superconductivity, University of Houston, Texas, 77204-5002, USA*
[c]*Verna and Marrs McLean Department of Biochemistry and Molecular Biology, Baylor College of Medicine, Houston, Texas, 77030, USA*
[d]*Laboratoire de Chimie Inorganique et Bioinorganique, Ecole Polytechnique Fédérale de Lausanne, EPFL-BCH, CH-1015, Lausanne, Switzerland*

† Electronic supplementary information (ESI) available: experimental and instrumentational detail. See http://dx.doi.org/10.1039/b504435a

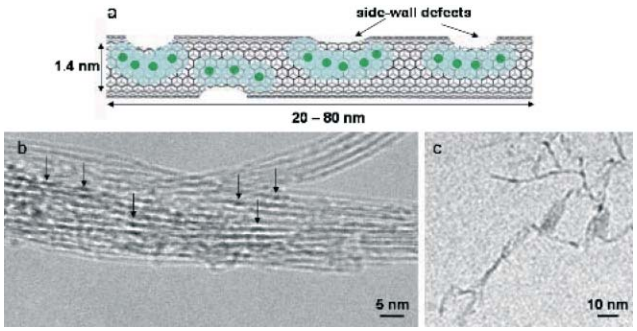

Fig. 1 (a) Depiction of a single US-tube loaded with hydrated Gd^{3+} ions. Gd^{3+}-ion loading is likely through side-wall defects created by cutting full-length nanotubes to produce bundled US-tubes (not to scale and Cl^- anion not shown). (b) HRTEM image of the $Gd^{3+}{}_n$@US-tubes showing the $Gd^{3+}{}_n$ clusters (arrows) formed within US-tubes as confirmed by EDS measurements. (c) Cryo-TEM image of $Gd^{3+}{}_n$@US-tubes from a 1% SDBS surfactant solution.

and further comparisons with commercial anhydrous $GdCl_3$ and Gd_2O_3 samples demonstrated that the confined Gd^{3+}-ion clusters more closely resemble $GdCl_3$. Thus, the absence of any Gd^{3+}-ion crystal lattice detectable by XRD may be attributed to the small cluster size (1 nm × 2–5 nm), the low gadolinium content (2.84% (m/m) from ICP) and/or the amorphous nature of the hydrated $Gd^{3+}{}_n$-ion clusters with their accompanying Cl^- counterions (Gd : Cl ratio 1 : 3 by XPS).

SQUID magnetic characterization of a gadonanotube sample is shown in Fig. 2, where the temperature dependence of magnetic susceptibility both at ZFC and FC fit well as Curie–Weiss law. Under the same conditions, an empty US-tube control sample showed no observable magnetization (Supplementary, Fig. S3). A linear least-square fit of Fig. 2 yielded values of $\mu_{eff} = 6.78\ \mu_B$, $\theta = -1.32$ K (5 K $< T <$ 300). The magnetization curve recorded at 5 K (inset) showed the absence of magnetic saturation even at strong fields while the magnetization curves plotted against H/T (Supplementary, Fig. S4) superimpose at higher temperatures. These magnetization data, in conjunction with the HRTEM images, are consistent with superparamagnetic clusters of confined Gd^{3+} ions at the high temperatures,[13] while at 5 K, features very similar to those observed in other nanoscalar spin-glass-like systems are present.[14,15] The confined $Gd^{3+}{}_n$-ion clusters may also induce superparamagnetism in the US-tube sample by way of magnetic proximity effects similar to those proposed for meteoritic graphite.[16]

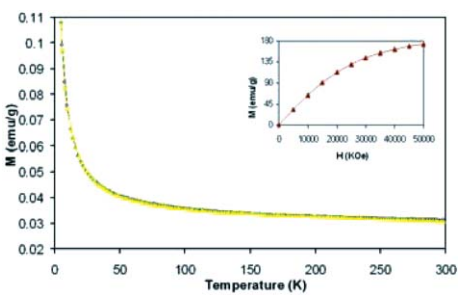

Fig. 2 Magnetization (ZFC + FC) *vs.* temperature plot for the $Gd^{3+}{}_n$@US-tubes measured at an applied field of 1000 Oe, along with an empirical linear least square fit. Inset: Magnetization curve of the same sample at 5 K. Lines between the data points are to guide the eyes.

Single-point relaxation measurements were performed on various $Gd^{3+}{}_n$@US-tube samples and controls at 60 MHz/40 °C. The longitudinal relaxation rates (R_1) were obtained by the inversion recovery method at pH = 7.0 and the longitudinal relaxivity (r_1) was obtained by $(T_1^{-1})_{obs} = (T_1^{-1})_d + r_1[Gd^{3+}]$, where T_{1obs} and T_{1d} are the relaxation times in seconds of the sample and the matrix (aqueous surfactant solution) respectively, and $[Gd^{3+}]$ is the Gd concentration in mM.

The absence of free (non-encapsulated) Gd^{3+} ion in the sample was confirmed by measuring the proton relaxivities of the solutions at 60 MHz before and after the addition of the ligand, $TTHA^{6-}$ (pH = 7). The details are given in the Supplementary Information.

Upon completion of the relaxation rate measurements, the Gd-content of the sample solution was determined by ICP-OES to calculate the relaxivity. The ICP-OES measurements were performed in-house at Rice University and independently confirmed at a commercial micro-analytical laboratory (Galbraith Laboratories, Inc); agreement was within 5%. The results of the relaxation rate measurements and relaxivity calculations are given in Table 1. It is clear from the table that the $Gd^{3+}{}_n$@US-tube samples significantly reduced the relaxation rates relative to pure surfactant solution or unloaded US-tubes. Comparing the relaxivity values of the $Gd^{3+}{}_n$@US-tube sample with $[Gd(H_2O)_8]^{3+}$, it is interesting to note that r_1 of aquated Gd^{3+} is 20 times lower at 60 MHz/40 °C than for the Gd_n^{3+}@US-tube sample. Thus, the relaxivity obtained for the $Gd^{3+}{}_n$@US-tube sample of $r_1 \sim 170\ mM^{-1}\ s^{-1}$ is nearly 40 times greater than any current Gd^{3+}-based oral or ECF CA, such as $[Gd(DTPA)(H_2O)]^{2-}$ with $r_1 \sim 4\ mM^{-1}\ s^{-1}$.[1] It is also nearly 8 times greater than ultrasmall superparamagnetic iron oxide (USPIO) contrast agents with $r_1 \sim 20\ mM^{-1}\ s^{-1}$.[17] We observed small variability in the relaxivity values of different batches of $Gd^{3+}{}_n$@US-tube samples and different surfactants used, but the order of magnitude reported in Table 1 was always the same ($r_1 = 159\ mM^{-1}\ s^{-1}$ to $179\ mM^{-1}\ s^{-1}$).

The measurement of proton relaxivity for a $Gd^{3+}{}_n$@US-tube sample in 1% SDBS solution as a function of the magnetic field is presented in Fig. 3. This Nuclear Magnetic Relaxation Dispersion (NMRD) profile was recorded for an aqueous solution of $Gd^{3+}{}_n$@US-tubes in a 1% SDBS solution at 37 °C. Also presented, for comparative purposes, are data for one of the commercially-available MRI CAs, $[Gd(DTPA)(H_2O)]^{2-}$, presently in clinical use. For any magnetic field in Fig. 3, the relaxivity for the $Gd^{3+}{}_n$@US-tubes is remarkably larger than for the clinical CA. This is true at the standard MRI field strength (nearly 40 times larger) for clinical imaging of 20–60 MHz ($170\ mM^{-1}\ s^{-1}$ *vs.* $4.0\ mM^{-1}\ s^{-1}$), but is even more pronounced (nearly 90 times larger) at very low fields such as 0.01 MHz ($635\ mM^{-1}\ s^{-1}$ *vs.* $7.0\ mM^{-1}\ s^{-1}$). In this regard, microtesla MRI imaging technologies would especially benefit from low-field, high efficacy

Table 1 Proton relaxivities, r_1, ($mM^{-1}\ s^{-1}$) of various sample solutions at 60 MHz and 40 °C

Sample	C_{Gd} (ppm)	C_{Gd} (mM)	T_1 (ms)	R_1 (s^{-1})	R_{1d} (s^{-1})	r_1 ($mM^{-1}\ s^{-1}$)
$Gd^{3+}{}_n$@US-tubes[a]	7	0.044	127.3	7.85	0.25	173
$Gd^{3+}{}_n$@US-tubes[b]	7.8	0.049	120.6	8.29	0.24	164
US-tubes[a]	—	—	2050	0.48	0.25	—
$[Gd(H_2O)_8]^{3+}$	313	1.99	59.0	16.95	0.24	8.4

[a] 1% SDBS surfactant solution. [b] 1% pluronic F98 surfactant solution.

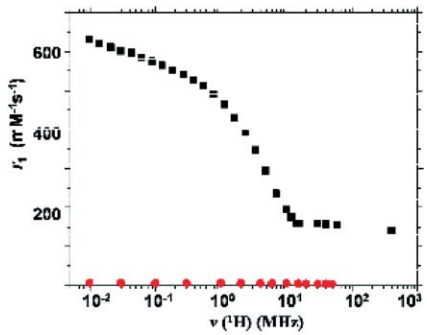

Fig. 3 NMRD profile measured on $Gd^{3+}{}_n$@US-tubes in a 1% SDBS solution (c_{Gd} = 0.044 mM; T = 37 °C) (black). For comparative purposes, data for the commercially-available CA, $[Gd(DTPA)]^{2-}$ are also shown (red).

contrast agents derived from gadonanotube synthons.[18] Recently it has been shown that a related nanostructural material, the gadofullerenes, can also exhibit large relaxivities ($\leqslant$ 80 mM^{-1} s^{-1}).[3,4,19] In this case, the increase in relaxivity results mainly from aggregation and the subsequent three-order-of-magnitude increase in τ_R, the rotational correlation time.[20] In the $Gd^{3+}{}_n$@US-tubes case, however, aggregation is not a contributing factor, since DLS measurements on the NMRD sample solution showed the hydrodynamic diameter of $Gd^{3+}{}_n$@US-tubes to be 20–80 nm, in good agreement with the Cryo-TEM images of Fig. 1c. Furthermore, the gadolinium centers in $Gd_n{}^{3+}$@US-tubes have access to water molecules (for Gd^{3+}–OH_2 bonding), since carbon nanotubes are known to be good transporters of water[21] and protons,[22] whereas the centers in gadofullerenes do not have this access. From a practical point of view, the rate of proton exchange is especially important, since it contributes to the proton relaxivity.[2] The present gadonanotubes, with their $Gd^{3+}{}_n$ clusters, are the first gadolinium CA materials where superparamagnetic metal centers have access to many coordinated/exchanging water molecules per Gd^{3+} ion. This unique situation could underlie the unprecedently large proton relaxivities exhibited by the $Gd^{3+}{}_n$@US-tubes. Indeed, these large relaxivities argue convincingly for confined, internally-loaded $Gd^{3+}{}_n$-ion clusters, since a highly-unusual metal-ion environment must be presumed to produce such extreme relaxivities.

NMRD measurements provide a valuable tool for separating the different relaxation mechanisms and dynamic processes influencing the relaxivity. In addition to the exceptionally large relaxivity values obtained for the gadonanotubes, the shape of the NMRD curve is also considerably different from that reported so far for any other Gd^{3+}-based system. In particular, the relaxivities are continuously decreasing with increasing magnetic field at proton Larmor frequencies below 1 MHz, in contrast to the usual Gd^{3+} CAs which present constant values at these low fields. Even more remarkable is the finding that at high magnetic fields ($>$ 60 MHz), the relaxivities remain practically constant, whereas a strong decrease is observed for the usual Gd^{3+} CAs. This phenomenon is particularly important, given the current tendency to develop MRI scanners of higher and higher fields, where the contrast enhancing effect of traditional contrast agents drops off. Currently, the most efficient T_1 agents show a typical high-field relaxivity peak centered around 30–40 MHz,[1] characteristic of slow rotation with maximum relaxivities of 40–50 mM^{-1} s^{-1}. Above this frequency, the relaxivity quickly vanishes to very small values. In this respect, gadonanotubes may represent a significant breakthrough in contrast agent design for high-field imaging.

The observed paramagnetic relaxation rate enhancement is related to various microscopic properties, the three most important being the proton/water exchange rate, the rotational correlation time, and the relaxation rate of the Gd^{3+} electron spin. For usual Gd^{3+} chelate compounds, this relation is described by the Solomon–Bloembergen–Morgan theory.[1] This theory is unable to predict the observed shape of the NMRD profile in Fig. 3 and thus, SBM theory does not appear appropriate for gadonanotubes. Clearly, further investigations are needed in order to explain both the extremely large relaxivities and the magnetic-field dependency of the proton relaxivities for the gadonanotubes and possibly other nanoscalar MRI CA materials, as well.

The work was supported by the NIH (Grant 1-R01-EB000703), the Robert A. Welch Foundation (Grants C-0627 and C-0109), the NCRR (NCRRP41RR02250), the Swiss National Science Foundation and Office for Education and Science (OFES). Part of this work was carried out in the frame of the EC COST Action D18 and the European-founded EMIL programme (LSHC - 2004 – 503569).

Notes and references

1 A. E. Merbach, E. Toth, Editors, *The Chemistry of Contrast Agents in Medical Magnetic Resonance Imaging*, John Wiley and Sons, Chichester, 2001.
2 P. Caravan, J. J. Ellison, T. J. McMurry and R. B. Lauffer, *Chem. Rev.*, 1999, **99**, 2293.
3 H. Kato, Y. Kanazawa, M. Okumura, A. Taninaka, T. Yokawa and H. Shinohara, *J. Am. Chem. Soc.*, 2003, **125**, 4391.
4 R. D. Bolskar, A. F. Benedetto, L. O. Husebo, R. E. Price, E. F. Jackson, S. Wallace, L. J. Wilson and J. M. Alford, *J. Am. Chem. Soc.*, 2003, **125**, 5471.
5 C. R. Martin and P. Kohli, *Nat. Rev. Drug Discovery*, 2003, **2**, 29.
6 Z. Gu, H. Peng, R. H. Hauge, R. E. Smalley and J. L. Margrave, *Nano Lett.*, 2002, **2**, 1009.
7 Y. A. Mackeyev, J. W. Marks, M. G. Rosenblum and L. J. Wilson, *J. Phys. Chem. B*, 2005, **109**, 5482.
8 M. Monthioux, *Carbon*, 2002, **40**, 1809.
9 N. W. S. Kam, T. C. Jessop, P. A. Wender and H. Dai, *J. Am. Chem. Soc.*, 2004, **126**, 6850.
10 Q. Lu, J. M. Moore, G. Huang, A. S. Mount, A. M. Rao, L. L. Larcom and P. C. Ke, *Nano Lett.*, 2004, **4**, 2473.
11 C. Journet, W. K. Maser, P. Bernier, A. Loiseau, M. Lamy de la Chapells, S. Lefrant, P. Deniard, R. Lee and J. E. Fischer, *Nature*, 1997, **388**, 756.
12 A. Hashimoto, H. Yorimitsu, K. Ajima, K. Suenaga, H. Isobe, J. Miyawaki, M. Yudasaka, S. Iijima and E. Nakamura, *Proc. Natl. Acad. Sci. USA*, 2004, **101**, 8527.
13 C. P. Bean and J. D. Livingston, *J. Appl. Phys.*, 1959, **30**, 120S.
14 B. Martinez, X. Obradors, L. Balcells, A. Rouanet and C. Monty, *Phys. Rev. Lett.*, 1998, **80**, 181.
15 P. Z. Si, I. Skorvanek, J. Kovac, D. Y. Geng, X. G. Zhao and Z. D. Zhang, *J. Appl. Phys.*, 2003, **94**, 6779.
16 J. M. D. Coey, M. Venkatesan, C. B. Fitzgerald, A. P. Douvalis and I. S. Sanders, *Nature*, 2002, **420**, 156.
17 S. Mornet, S. Vasseur, F. Grasset and E. Duguet, *J. Mater. Chem.*, 2004, **14**, 2161.
18 R. McDermott, S. Lee, B. ten Haken, A. H. Trabesinger, A. Pines and J. Clarke, *Proc. Natl. Acad. Sci. USA*, 2004, **101**, 7857.
19 E. Toth, R. D. Bolskar, A. Borel, G. Gonzalez, L. Helm, A. E. Merbach, B. Sitharaman and L. J. Wilson, *J. Am. Chem. Soc.*, 2005, **127**, 799.
20 B. Sitharaman, R. D. Bolskar, I. Rusakova and L. J. Wilson, *Nano Lett.*, 2004, **4**, 2373.
21 G. Hummer, J. C. Rasalah and J. P. Noworyta, *Nature*, 2001, **414**, 188.
22 C. Dellago, M. M. Naor and G. Hummer, *Phys. Rev. Lett.*, 2003, 90105902/1.